DOI: 10.1002/asia.200900217

Multianalyte Electrochemical Biosensor Based on Aptamer- and Nanoparticle-Integrated Bio-Barcode Amplification

Xuemei Li, Jianping Xia, Wei Li, and Shusheng Zhang*[a]

Abstract: In the present work, a signal-on electrochemical sensing strategy for the simultaneous detection of adenosine and thrombin is developed based on switching structures of aptamers. An Au electrode as the sensing surface is modified with two kinds of thiolated capture probes complementary to the linker DNA that contains either an adenosine aptamer or thrombin aptamer. The capture probes hybridize with their corresponding linker DNA, which has prehybridized with the reporter DNA loaded onto the gold nanoparticles (AuNPs). The AuNP contained two kinds of bio-barcode DNA: one is complementary to the linker DNA (reporter), whereas the other is not (signal) and is tagged with different metal sulfide nanoparticles. Thus a "sandwich-type" sensing interface is fabricated for adenosine and thrombin. With the introduction of adenosine and thrombin, the aptamer parts bind with their targets and fold to form the complex structures. As a result, the bio-barcoded AuNPs are released into solution. The metal sulfide nanoparticles are measured by anodic stripping voltammetry (ASV), and the concentrations of adenosine and thrombin are proportional to the signal of either metal ion. With the dual amplification of the bio-barcoded AuNP and the preconcentration of metal ions through ASV technology, detection limits as low as 6.6×10^{-12} M for adenosine and 1.0×10^{-12} M for thrombin are achieved. The sensor exhibits excellent selectivity and detectability in biological samples.

Keywords: adenosine · aptamers · nanostructures · sensors · thrombin

Introduction

Aptamers are molecular receptors made of single- and/or double-stranded oligonucleotides, which are obtained from large combinatorial libraries by an in vitro process of systematic evolution of ligands by exponential enrichment (SELEX),[1,2] capable of specifically binding a variety of molecules. As a result of their inherent selectivity, affinity, stability, and flexibility, aptamers have become increasingly important molecular tools for diagnostics and therapeutics. In particular, aptamer-based biosensors (aptasensors) possess unprecedented advantages compared with biosensors using natural receptors such as antibodies and enzymes.[3]

Recently, a number of aptasensors have been developed, including optical,[4,5] electrochemiluminescene (ECL),[6] surface plasmon resonance (SPR),[7] colorimetry,[8,9] and electrochemistry.[10,11] The combination of the advantages of electrochemical methods with the specific recognition properties of the aptasensors has enabled the investigations on electrochemical aptasensors, the detection of targets including small molecules,[12–14] proteins,[15,16] and cells.[17] Wu et al. reported a reusable electrochemical sensing platform for highly sensitive detection of small molecule adenosine based on structure-switching signaling aptamers tagged with the redox probe ferrocene.[18] Willner's group designed a label-free and reagentless aptasensor for the selective analysis of adenosine based on a reagentless aptamer/partly complementary strand aptamer/target-sensing interface using an ion-selective field-effect transistor (ISFET).[19] Recently, Yu's group presented a new class of DNA conformational switches (deoxyribosensors) for the highly sensitive detection and quantitation of the plasma protein thrombin.[20]

Most electrochemical aptasensors described above have been constructed mainly based on the conformational change of the aptamers induced by the specific target binding.[21–23] Different from the existing strategies with the surface-confined aptamers as the probes for electrochemical

[a] Dr. X. Li, J. Xia, W. Li, Prof. Dr. S. Zhang
Key Laboratory of Eco-Chemical Engineering, Ministry of Education
College of Chemistry and Molecular Engineering
Qingdao University of Science and Technology
Qingdao 266042 (China)
Fax: (+86) 532-84022750
E-mail: shushzhang@126.com

Supporting information for this article is available on the WWW under http://dx.doi.org/10.1002/asia.200900217.

target sensing, Lu et al. described a new and relatively general approach to the electrochemical aptasensors by using the aptamer–complementary DNA (cDNA) oligonucleotides as the probes.[24] Recently, the application of nanomaterials has provided a novel approach to develop truly label-free, high-sensitivity sensors. For example, a single-walled carbon nanotube field-effect transistor (SWCNT-FET) device was fabricated to monitor the aptamer–protein binding affinity processes. The aptamer-modified CNT-FET could detect immunoglobulin E (IgE) at a limit of detection (LOD) as low as 250 pM.[16]

Multiple-analyte detection has made great progress through the development of immunoassays[25,26] and hybridization assays[27–31] that permit simultaneous determination of multiple antigen and DNA targets. A limited amount of research has reported on the simultaneous detection of multiple small molecules or proteins. Hansen et al. reported the coupling of aptamers with the coding and amplification features of inorganic nanocrystals to offer a sensitive and selective simultaneous bioelectronic detection of several protein targets.[32] Very recently Elbaz et al. demonstrated the parallel electrochemical analysis of two analytes in solutions or on surfaces by using a bifunctional aptamer.[33] Du et al. reported a multifunctional label-free electrochemical aptasensor for parallel detection both of adenosine triphosphate (ATP) and thrombin using electrochemical impedance spectroscopy (EIS) measurements.[34] However, such a sensing interface was not suitable for the type of simultaneous detection in which multitargets were in one sample. Multianalyte aptamer-based devices are highly desired for measuring a large panel of disease markers present at ultralow levels during early stages of the disease.

In this present work, an electrochemical sensing strategy for simultaneous detection of adenosine and thrombin was developed based on switching structures of aptamers from DNA/DNA duplex to DNA/target complex upon binding to their target molecules. We used gold nanoparticles (AuNPs) containing two DNA bio-barcodes to reduce cross-reaction and offered a significant amplification as a result. The introduction of CdS and PbS nanoparticles enhanced the sensitivity with preconcentration of the metal ions through anodic stripping voltammetry (ASV) technology. With this sensing interface, adenosine and thrombin could be detected with high sensitivity and selectivity, even in a serum sample.

Abstract in Chinese:

基于适体结构变化提出了一种同时检测腺苷和凝血酶分子的电化学传感器 在金电极上固定两种巯基修饰的探针 DNA，它们分别与含有腺苷适体和凝血酶适体的连接 DNA 的一部分互补 该连接 DNA 已经与金纳米粒子表面的报告 DNA 进行了预杂交，然后探针 DNA 与各自对应的连接 DNA 杂交 金纳米粒子表面固定了两种不同的 DNA，一种与连接 DNA 互补，另外一种不互补，只是起到连接不同的金属硫化物纳米粒子的作用 至此，一个检测腺苷和凝血酶分子的“三明治”式的结构建立起来了 当有腺苷和凝血酶分子存在的时候，适体部分发生弯曲与各自的目标分子形成复杂结构，同时，连接有金属硫化物纳米粒子的金纳米粒子从电极表面脱落，进入到溶液中 对溶液中的金属硫化物纳米粒子采用阳极溶出伏安法（ASV）进行测定，腺苷和凝血酶分子的浓度与各自对应的金属硫化物的溶出信号成正比 经过纳米粒子-金属硫化物纳米粒子和 ASV 对金属离子的富集技术两重放大作用，检测腺苷的检测限为 6.6×10^{-12} M；检测凝血酶的检测限为 1.0×10^{-12} M 该传感器在生物样品中表现出了良好的选择性和良好的检测能力

Results and Discussion

Experimental Principle of a Sensing System Based on Aptamers and Bio-Barcodes

To investigate an electrochemical sensing platform for simultaneous detection of small molecules and protein, the adenosine and thrombin aptamers were studied as model systems. The system contained thiolated capture probe DNA sequences (S_1 and S_2), linker DNA sequences (S_3 and S_4), AuNP-linked DNA sequences as reporter probes (S_5 and S_6), and adenosine and thrombin as the model analytes, respectively. These sequences are presented in Table 1. Each linker DNA contained an aptamer fragment (designated in Table 1 by normal font) and an extension (designated by italic and bold formatting). The bold part of the linker hybridized to the thiolated capture DNA immobilized on the electrode, whereas the italic part and a small fraction of the normal part of the linker hybridized to the reporter probe functionalized with AuNPs. The fabrication and experimental principle of the sensing platform is shown in Scheme 1. The surface of a gold electrode was firstly modified with directly electrodeposited AuNPs and 3′-thiol-modified capture DNA strands were immobilized on the resulting electrode surface by means of sulfur–gold affinity. The linker DNA sequences, which were prehybridized with the barcoded DNA, were then dually hybridized with the immobilized capture strands, thereby forming a “sandwich” assay.

An aptamer can bind tightly and specifically to a variety of target molecules to form a tertiary complex with a binding constant greater than that of the part-DNA duplex designed in this work. In the presence of adenosine and thrombin, the aptamer parts bound to their respective targets and folded to form the complex structure. As a result, only the italic part on the linker DNA was left to bind to the probe sequence, which was unstable at room temperature, and reporter DNA together with AuNP was released into the solution. The nanoparticles in the solution were dissolved by the addition of HNO_3 and the amount and identity of the dissolved metal ions were determined by stripping voltammetry.

In our previous report,[35] it was found that there were 127 single strands per AuNP by thiolated DNA by means of gold–sulfur affinity; the ratio of reporter probe and signal probe was 1:4. Compared with AuNP labeled with all complementary reporter DNA, the probe density was low. This enabled one AuNP to be labeled with one target, thereby offering a significant amplification. When metal sulfide nanoparticles were dissolved from the hybrids, a secondary amplification was performed by preconcentration of metal ions through ASV technology.

Table 1. DNA sequences used in the current study.

Name	Sequence	Description
capture DNA (S_1)	3′-HS-$(CH_2)_6$-**TGA-GTA-GAC-ACT**-5′	thiolated probe immobilized on Au electrode
capture DNA (S_2)	3′-HS-$(CH_2)_6$-**GTA-CTG-CGA-CTT**-5′	thiolated probe immobilized on Au electrode
linker DNA (S_3)	5′-**ACT-CAT-CTG-TGA**-*AGA-GA*A-CCT-GGG-GGA-GTA-TTG-CGG-AGG-AAG-GT-3′	44-base sequence that contains complementary sequences to both S_1 (bold) and S_5 (italic), as well as adenosine aptamer (normal font)
linker DNA (S_4)	5′-**CAT-GAC-GCT-GAA**-*CTC-ACA-GTC-CGT*-GGT-AGG-GCA-GGT-TGG-GGT-GAC-T-3′	46-base sequence that contains complementary sequences to both S_1 (bold) and S_5 (italic), as well as thrombin aptamer (normal font)
reporter DNA (S_5)	3′-*TCT-CTT-GGA-CCC*-$(CH_2)_6$-SH-5′	thiolated probe loaded on AuNP and complementary to S_3
reporter DNA (S_6)	3′-*GAG-TGT-CAG-GCA*-$(CH_2)_6$-SH-5′	thiolated probe loaded on AuNP and complementary to S_4
signal DNA (S_7)	3′-NH_2-TTT-TTT-TT-$(CH_2)_6$-SH-5′	thiolated probe loaded on AuNP

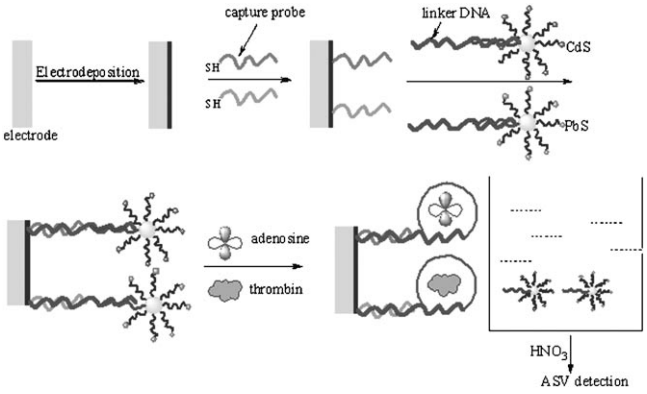

Scheme 1. Schematic representation of the sensing interface. The aptamers bound to their targets folded to form the complex structure, and metal sulfide nanoparticles together with AuNPs were released into solution, which resulted in a decrease in the current as monitored by ASV.

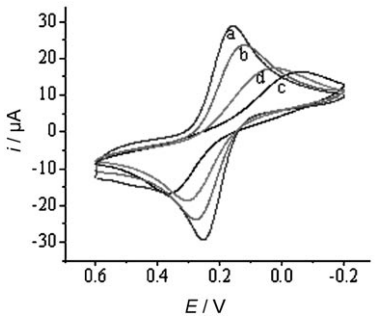

Figure 1. Faradaic impedance spectra corresponding to Au electrodes a) modified with AuNPs, b) after immobilization of probes 1 and 2, c) after hybridization with linker DNA and bio-barcoded AuNPs, and d) after treatment with 1.8×10^{-10} M of adenosine and 1.6×10^{-11} M of thrombin. The data were recorded in the presence of $[Fe(CN)_6]^{3-}$/$[Fe(CN)_6]^{4-}$ (2.5 mM) as redox label and, upon application of the biasing potential 0.21 V, by applying 5 mV alternate voltage in the frequency range of 50 mHz to 10 kHz. Data were recorded in phosphate buffer solution (PBS; 10 mM) that included KCl (100 mM) at pH 7.4. The electrode area after AuNP deposition is 30.9 mm^2.

Characterization of the Modified Electrode

The Au electrodes with and without AuNP deposition have been characterized by SEM and atomic force microscopy (AFM) in our previous work.[36] The active surface areas of the AuNP-modified Au electrode was 3 times that of the bare Au electrode. The assembly of nucleic acids on electrodes and the formation of double-stranded DNA on the support was measured using both Faradaic impedance spectroscopy (FIS) and CV. Figure 1 shows a Nyquist plot of impedance for Au electrodes a) modified with AuNPs, b) after immobilization of probes 1 and 2, c) after hybridization with linker DNA and bio-barcoded AuNPs, and d) after treatment with 1.8×10^{-10} M of adenosine and 1.6×10^{-11} M of thrombin. The charge-transfer resistance (R_{ct}) of the Au electrode with AuNP deposition was around 0 Ω. After immobilization of probes 1 and 2, the value of R_{ct} increased to 1189 Ω. The increase in R_{ct} is due to the immobilization of negatively charged oligodeoxynucleotide (ODN) probes on the electrode surface, thereby resulting in a negatively charged interface that electrostatically repels the negatively charged redox probe $[Fe(CN)_6]^{3-}$/$[Fe(CN)_6]^{4-}$ and inhibits interfacial charge transfer.[37] After hybridization with linker DNA and capture DNA, the value of R_{ct} was further increased to 5868 Ω, owing to the large amount of DNA linked on the AuNPs. After treatment of adenosine and thrombin, the interfacial electron resistance decreased, which was consistent with the removal of the negative charge from the electrode by the removal of signal DNA. The surface coverage of the capture DNA was 5.5×10^{12} molecules cm^{-2}, and the surface density of the aptamer and nucleic acids functionalizing the nanoparticles was 1.2×10^{14} molecules cm^{-2} (see Figure S1 in the Supporting Information).

The modified electrodes were further investigated by CV (Figure 2). The CV response showed results consistent with those of FIS. The peak current of $[Fe(CN)_6]^{3-}$/$[Fe(CN)_6]^{4-}$ on the Au electrode with AuNP deposition was largest. Upon immobilization of the capture probes and the subsequent 6-mercapto-1-hexanol (MCH) regularization on the gold surface, the peak current decreased. The CV response evidently decreased after the sandwich sensing interface formed and then increased after treatment of adenosine and

CHEMISTRY
AN ASIAN JOURNAL

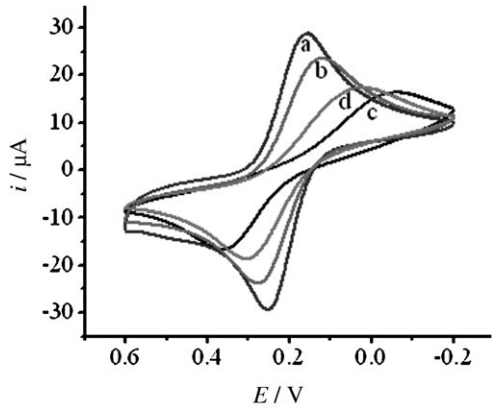

Figure 2. Cyclic voltammograms corresponding to Au electrodes a) modified with AuNPs, b) after immobilization of probes 1 and 2, c) after hybridization with linker DNA and bio-barcoded AuNPs, and d) after treatment with 1.8×10^{-10} M of adenosine and 1.6×10^{-11} M of thrombin. The data were recorded in the presence of $[Fe(CN)_6]^{3-}/[Fe(CN)_6]^{4-}$ (2.5 mM) as redox label.

thrombin. All these results indicated that the sensing architecture was fabricated successfully.

Simultaneous Signal-On Detection of Adenosine and Thrombin

The introduction of adenosine and thrombin in different concentrations to the sensing interface induced different degrees of removal of the PbS and CdS nanoparticles. The metal sulfide crystals released into the solution were measured by ASV after dissolving them with HNO_3. The position and size of each peak reflected the identity and the concentration of the corresponding adenosine and thrombin targets to allow convenient multitarget quantification in one sample.

Figure 3 shows the ASV response for the dissolved PbS and CdS after different concentrations of adenosine and thrombin were introduced. From the ASV response for the dissolved PbS and CdS after different concentrations of adenosine and thrombin were introduced, one can see how it is affected by sample mixtures that contain increasing levels of

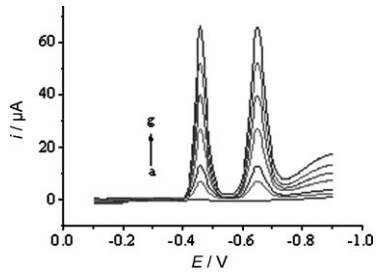

Figure 3. ASV analysis of the nanoparticles in the solution after the treatment of adenosine and thrombin. The concentrations of adenosine: a) 0, b) 2.0×10^{-10}, c) 4.0×10^{-10}, d) 8.0×10^{-10}, e) 1.2×10^{-9}, f) 1.6×10^{-9}, and g) 2.0×10^{-9} M. The concentrations of thrombin: a) 0, b) 2.0×10^{-11}, c) 4.0×10^{-11}, d) 8.0×10^{-11}, e) 1.2×10^{-10}, f) 1.6×10^{-10}, and g) 2.0×10^{-10} M.

the two targets. The lead and cadmium peaks were well defined and proportional to the concentration of corresponding targets, thus indicating minimal cross-interference. It illustrated that mixtures of two targets can be analyzed in a quantitative fashion.

Figure 4 represents the relationship between the currents and adenosine or thrombin concentrations. The graph can be also considered as a calibration graph because it gives

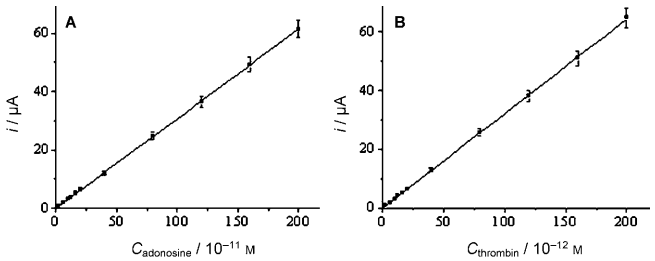

Figure 4. The linear relationship between the peak current and A) adenosine and B) thrombin concentration.

the relationship between the sensor signal and the concentrations of the target adenosine and thrombin. The currents increased continuously as a function of adenosine and thrombin concentrations in the range of 2.0×10^{-11} to 2.0×10^{-9} M and 2.0×10^{-12} to 2.0×10^{-10} M, respectively. The regression equation for adenosine was $y=0.3215x-0.0343$ (y was the current, μA; x was the concentration of adenosine, 10^{-11} M), and the regression coefficient of the linear curve was 0.9999. The regression equation for thrombin was $y=0.3070x+0.0448$ (y was the current, μA; x was the concentration of thrombin, 10^{-12} M), and the regression coefficient of the linear curve was 0.9998. Detection limits of 6.6×10^{-12} and 1.0×10^{-12} M of adenosine and thrombin, respectively, can be estimated using 3σ.

For comparison, a signal-off simultaneous detection of adenosine and thrombin has also been investigated by detecting the metal sulfide nanoparticles remaining at the surface (see the Supporting Information for details). The currents decreased continuously as a function of adenosine and thrombin concentrations in the range of 2.0×10^{-11} to 1.8×10^{-10} M and 2.0×10^{-12} to 1.6×10^{-11} M, respectively. Detection limits of 7.8×10^{-12} and 1.2×10^{-12} M of adenosine and thrombin, respectively, can be estimated using 3σ. In a comparison with the results of the signal-off detection, the signal-on method had lower detection limits and wider linear ranges for the detection of adenosine and thrombin.

In our previous report, a detection limit of 1.8×10^{-10} M for adenosine was achieved with the enhancement effect of AuNPs and $[Ru(NH_3)_6]^{3+}$ as the redox label.[36] In the present study, by taking advantage of dual amplification effects of multifunctional encoded AuNPs and the preconcentration process of metal ions performed by ASV technology, the detection limit for adenosine was lower than that of our previous report.[36] The detection limit obtained using the present sensing system is lower than the literature value of single-

target analysis[11,18–20,24] and dual-analyte detection[32,34,38] achieved using aptamer-based sensors. Moreover, a series of eight repetitive measurements of the 6.0×10^{-11} M adenosine and 6.0×10^{-12} M thrombin solution yielded reproducible cadmium and lead peaks with coefficients of deviation of 8.4 and 6.3%, respectively, thereby reflecting the reproducibility of the protocol. The recoveries of different concentrations of adenosine and thrombin were of 82.2–115.4 and 85.3–118.6%, respectively (see Table S1 in the Supporting Information).

Selectivity of the Sensing Interface

The selectivity of this technique was based on the high affinity between aptamers and their target molecules. The experiments in terms of interaction specificity and absence of nonspecific binding were carried out to investigate whether there is any cross-interference. The sensing interface was treated with the solution that contained different targets. The results of the cross-reaction studies are presented in Figure S3 in the Supporting Information. After treatment with the solution that contained adenosine alone, only the corresponding cadmium peak was observed in the voltammogram and no lead peak current was observed (Figure S3a). Similar selectivity was obtained for thrombin (Figure S3b). These results showed that the aptamers were specific to their target molecules and our technique could simultaneously determine two targets in a single sample.

Guanosine, cytidine, and uridine belong to the nucleosides family. Cytidine and uridine were examined to serve as a control to assess the specificity of the aptamer-modified gold electrodes for the detection of adenosine. Guanosine was not tested because of its poor solubility at room temperature. Bovine serum albumin (BSA) and lysozyme were also chosen as a control for thrombin. As can be seen from Figure S4 in the Supporting Information, even with concentrations as high as 2.0×10^{-10} M of cytidine and uridine, and 2.0×10^{-11} M of BSA and lysozyme, no evidence for binding of these noncognate proteins to the sensors was detected, as compared with the case of adenosine and thrombin.

Application of the Aptasensor in Biological Assay

It has been reported that adenosine concentration in normal human blood ranges between 0.05 and 0.1 μM.[39,40] And the physiological concentrations of thrombin in resting and activated blood range from low nanomolar to low micromolar amounts.[41] Given the very high sensitivity of the aptasensor, the serum sample was diluted 1000 times before analysis with the present method. Blood samples prepared from six patients were analyzed by this sensor assay. The results are listed in Table 2. For all six samples tested, adenosine was observed in the range of 55.2 to 90.8 nM. Thrombin was not detectable in two of the six samples because thrombin is not present in the blood and plasma of healthy subjects when coagulation is not occurring.[42] Although no thrombin was observed in those two samples, low nanomolar levels of thrombin were detected in the other four plasma samples. Given that the blood samples employed were patient plasmas that might suffer from diseases known to be associated with coagulation abnormalities, some activation of the blood-clotting cascade may have occurred, thereby producing detectable levels of thrombin. These results demonstrated that the effect of nonspecific proteins and electrolytes in the original plasma on this sensor application might be negligible.

Table 2. The detection results of adenosine and thrombin in the plasma samples.

Sample	Adenosine [nM]	Thrombin [nM]
1	55.2	2.2
2	62.3	3.8
3	84.4	–
4	60.5	4.7
5	90.8	–
6	79.9	2.5

Conclusion

A multifunctional electrochemical sensing strategy for simultaneous detection of adenosine and thrombin was demonstrated. The design relies on the structure-switching properties of aptamers from DNA/DNA duplex to DNA/target complex upon binding to their target molecules. There are three advantages in our present work. Firstly, the use of AuNPs that contain two DNA bio-barcodes has reduced the degree of cross-reaction relative to single bio-barcode assays. Secondly, the introduction of CdS and PbS nanoparticles has enhanced the sensitivity in addition to the preconcentration of the metal ions. Thirdly, the detection method is a signal-on pattern. These three aspects lowered the detection limit of adenosine compared to that of our previous report.[36] Moreover, the sensor was suitable for the simultaneous detection of adenosine and thrombin in one sample, thereby providing a promising detection technique for both small molecules and protein, even in biological fluids.

Experimental Section

Chemicals

All oligonucleotides were designed according to the literature in the present study and were purchased from SBS Genetech Co., Ltd. (Beijing, China), and their sequences are presented in Table 1. Adenosine, cytidine, uridine, bovine serum albumin (BSA), and lysozyme were from Sigma (St. Louis, MO) and used without further purification. 6-Mercapto-1-hexanol (MCH), hexaammineruthenium(III) chloride (98%), erythro-9-(2-hydroxy-3-nonyl)adenine (EHNA, adenosine deaminase inhibitor), dipyridamole, α,β-methylene adenosine-5′-diphosphate, and disodium ethylenediaminetetraacetic acid (Na_2EDTA) were also purchased from Sigma. Tri(2-carboxyethyl)phosphine hydrochloride (TCEP, 98%) was purchased from Alfa Aesar (MA, USA). Other chemicals employed were all of analytical grade and double-distilled water (DDW) was used throughout. The human serum samples from six patients were provided by the Medical School Hospital of Qingdao University (Qingdao, China).

Preparation of AuNPs

Gold nanoparticles were prepared by citrate reduction of $HAuCl_4$ according to the literature.[9] Briefly, sodium citrate (10 mL, 38.8 mM) was immediately added to a solution of $HAuCl_4$ (100 mL, 1.0 mM) heated to reflux under stirring, and the mixture was kept boiling for another 15 min. The solution color turned wine red and was cooled to room temperature with continuous stirring. The sizes of the AuNPs were verified by transmission electron microsocopy (TEM) using a JEOL JEM-2000EX microscope (Japan). The AuNPs have average diameters of 20 nm (Figure S5 in the Supporting Information).

Preparation of PbS and CdS NPs

Nanoparticles of lead sulfide and cadmium sulfide were prepared according to the literature.[43] For the preparation of each of the two types of nanoparticles, mercaptoacetic acid (2 μL) was added to the respective metal chloride solution (100 mL, 1 mM) under vigorous stirring, and the pH was adjusted to 11 with NaOH (0.5 M). The solution was bubbled with nitrogen for 30 min, and Na_2S (50 mL, 1.34 mM) was added dropwise to the solution. The reaction was kept under bubbling nitrogen for 24 h. The resulting nanoparticles have average diameters of 10 nm as characterized by TEM (Figure S5 in the Supporting Information).

Preparation of Bio-Barcoded AuNPs Containing Metal Sulfide Nanoparticles

The process of signal and reporter DNA labeling was performed as follows.[44,45] The mixture of S_7 (4.3×10^{-11} mol) and S_5 or S_6 (3.0 nmol) was activated with acetate buffer (pH 5.2) and TCEP (1.5 μL, 10 mM) for 1 h, and then added to freshly prepared AuNPs (1 mL) and shaken gently overnight. Over the course of 16 h, the DNA–AuNP conjugates were aged in salts (0.1 M NaCl, 10 mM acetate buffer) for another 24 h. Excess reagents were removed by centrifuging the samples at 16000 rpm for 30 min. The red precipitate was washed, recentrifuged, and dispersed in buffer (1 mL) containing NaCl (300 mM) and tris(hydroxymethyl)aminomethane (Tris) acetate (25 mM, pH 8.2).

Preparation of bio-barcoded AuNPs containing metal sulfide nanoparticles was performed according to our previous report.[46] An imidazole solution (200 μL, 0.1 M, pH 6.8) was added to each of the prepared oligonucleotide-functionalized AuNP solutions (2.0 mL). After 30 min, *N*′-(3-dimethylaminopropyl)-*N*-ethylcarbodiimide (EDC) solution (100 μL, 0.1 M) and PbS or CdS (2.0 mL) colloid were added to the mixture and incubated at room temperature for 24 h with gentle shaking. Excess reagents were removed by centrifugation at 10000 rpm for 30 min. The precipitate was washed and then dispersed into water. The solution of bio-barcoded gold nanoparticles containing CdS or PbS NPs was stored at 4 °C for the hybridizations.

Gold Nanoparticle Deposition

The gold electrode was polished with alumina powder (0.05 μm) and soaked in an ultrasonic bath successively with distilled water, absolute alcohol, and distilled water for 5 min each. Then the gold electrode was dipped in piranha solution (H_2SO_4/H_2O_2, 7:3 v/v) for 5 min at 90 °C and electrochemically treated by cycling the potential between +0.1 and +1.5 V in 0.1 M H_2SO_4 until a stable gold oxide cyclic voltammogram was obtained. The pretreated electrodes were immersed into the $HAuCl_4$ solution (6.0 mM) containing KNO_3 (0.1 M), in which electrochemical deposition was conducted at −400 mV by using the single potential mode.

Capture DNA Immobilization and Hybridization on Gold Electrodes

Gold electrodes coated with AuNPs were immersed into an immobilization buffer (IB; Tris-HCl (20 mM)+NaCl (0.1 M)+$MgCl_2$ (5 mM) at pH 7.4) containing both capture probes (1.0×10^{-8} M) for 12 h. The DNA-modified electrodes were further treated with MCH (1 mM) for 2 h to obtain well-aligned DNA monolayers.

Linker DNA was preannealed with reporter probes loaded on AuNPs at 37 °C for 30 min in the hybridization buffer, and then the solution (4 μL) was placed on gold electrodes with DNA self-assembly monolayers (SAMs) for 1 h at room temperature. After hybridization, electrodes were extensively rinsed with washing buffer (Tris-HCl (10 mM) at pH 7.4) and dried under a stream of nitrogen prior to electrochemical characterization.

Simultaneous Electrochemical Detection of Adenosine and Thrombin

For the detection procedure, the sensing interface was immersed for 90 min into IB buffer that contained various concentrations of adenosine and thrombin. With the addition of HNO_3 (2.0 M, 135 μL), the metal sulfide nanoparticles in the IB solution were dissolved. The solution that contained the dissolved quantum dots were transferred into acetate buffer (1.8 mL, 0.10 M, pH 5.3) that contained mercury ions (0.01 gL^{-1}). ASV was conducted in a standard electrochemical cell using an electrochemical analyzer (CHI660C, CH Instruments, USA). The three-electrode setup consisted of a Pt-wire electrode as the counter electrode, an Ag/AgCl reference electrode, and an in situ formed mercury-film electrode (on a glassy carbon surface) generated as working electrode, by accumulation for 200 s at −1.4 V. After standing for 15 s, the stripping voltammetry was carried out between −1.0 and −0.1 V using anodic stripping voltammetry. CV and FIS were carried out in a degassed phosphate buffer solution (PBS, pH 7.4) that contained KCl (0.1 M) and $[Fe(CN)_6]^{3-}/[Fe(CN)_6]^{4-}$ (2.5 mM).

Treatment of Plasma Samples

Plasma samples were pretreated with salt solution (ammonium sulfate (2 M) and NaCl (0.1 M)) to avoid the formation of fibrin and the rapid sample clotting according to the previous reports.[47,48] Then the plasma sample (1.0 mL) was transferred to tubes that contained an equal volume of ice-cold stop solution (EHNA (120 μM), dipyridamole (20 mM), α,β-methylene adenosine-5′-diphosphate (60 mM), and Na_2EDTA (4.2 mM)). The mixture of blood and stop solution was then immediately centrifuged for 5 min at 10000 rpm at 4 °C. The plasma was removed and frozen at −70 °C until used. Adenosine and thrombin were measured after appropriate dilution and were calculated from the measured concentrations after correction for dilution.

Acknowledgements

This work was supported by the National Natural Science Foundation of China (nos. 20875052, 20775038), the Natural Science Foundation of Shandong Province (nos. Y2007B31, JQ200805), and the Outstanding Adult-Young Scientific Research Encouraging Foundation of Shandong Province (no. 2008BS05009).

[1] C. Tuerk, L. Gold, *Science* **1990**, *249*, 505–510.
[2] A. D. Ellington, J. W. Szostak, *Nature* **1990**, *346*, 818–822.
[3] S. P. Song, L. H. Wang, J. Li, C. H. Fan, J. L. Zhao, *TrAC Trends Anal. Chem.* **2008**, *27*, 108–117.
[4] V. Bagalkot, L. Zhang, E. Levy-Nissenbaum, S. Jon, P. W. Kantoff, R. Langer, O. C. Farokhzad, *Nano Lett.* **2007**, *7*, 3065–3070.
[5] Y. Y. Li, C. Zhang, B. S. Li, L. F. Zhao, X. B. Li, W. J. Yang, S. Q. Xu, *Clin. Chem.* **2007**, *53*, 1061–1066.
[6] J. Bai, H Wei, B. Li, L. Song, L. Fang, Z. Lv, W. Zhou, E. Wang, *Chem. Asian J.* **2008**, *3*, 1935–1941.
[7] S. J. Lee, B. S. Youn, J. W. Park, J. H. Niazi, Y. S. Kim, M. B. Gu, *Anal. Chem.* **2008**, *80*, 2867–2873.
[8] J. Liu, Y. Lu, *J. Am. Chem. Soc.* **2007**, *129*, 8634–8643.
[9] J. Liu, Y. Lu, *Nat. Protoc.* **2006**, *1*, 246–252.
[10] M. C. Rodriguez, A. N. Kawde, J. Wang, *Chem. Commu.* **2005**, 4267–4269.
[11] Y. Xiang, M. Xie, R. Bash, J. J. L. Chen, J. Wang, *Angew. Chem.* **2007**, *119*, 9212–9214; *Angew. Chem. Int. Ed.* **2007**, *46*, 9054–9056.
[12] X. L. Zuo, S. P. Song, J. Zhang, D. Pan, L. H. Wang, C. H. Fan, *J. Am. Chem. Soc.* **2007**, *129*, 1042–1043.
[13] Y. Du, B. Li, F. Wang, S. Dong, *Biosens. Bioelectron.* **2009**, *24*, 1979–1983.

[14] K. Feng, C. Sun, Y. Kang, J. Chen, J. H. Jiang, G. L. Shen, R. Q. Yu, *Electrochem. Commun.* **2008**, *10*, 531–535.
[15] Y. Xiao, A. A. Lubin, A. J. Heeger, K. W. Plaxco, *Angew. Chem.* **2005**, *117*, 5592–5595; *Angew. Chem. Int. Ed.* **2005**, *44*, 5456–5459.
[16] K. Maehashi, T. Katsura, K. Kerman, Y. Takamura, K. Matsumoto, E. Tamiya, *Anal. Chem.* **2007**, *79*, 782–787.
[17] J. K. Herr, J. E. Smith, C. D. Medley, D. H. Shangguan, W. H. Tan, *Anal. Chem.* **2006**, *78*, 2918–2924.
[18] Z. S. Wu, M. M. Guo, S. B. Zhang, C. R. Chen, J. H. Jiang, G. L. Shen, R. Q. Yu, *Anal. Chem.* **2007**, *79*, 2933–2939.
[19] M. Zayats, Y. Huang, R. Gill, C. A. Ma, I. Willner, *J. Am. Chem. Soc.* **2006**, *128*, 13666–13667.
[20] Y. C. Huang, B. Ge, D. Sen, H. Z. Yu, *J. Am. Chem. Soc.* **2008**, *130*, 8023–8029.
[21] R. Nutiu, Y. Li, *Chem. Eur. J.* **2004**, *10*, 1868–1876.
[22] J. S. Hartig, S. H. Najafi-Shoushtari, I. Gruene, A. Yan, A. D. Ellington, M. Famulok, *Nat. Biotechnol.* **2002**, *20*, 717–722.
[23] N. Rupcich, R. Nutiu, Y. Li, J. D. Brennan, *Angew. Chem.* **2006**, *118*, 3373–3377; *Angew. Chem. Int. Ed.* **2006**, *45*, 3295–3299.
[24] Y. Lu, X. Li, L. Zhang, P. Yu, L. Su, L. Mao, *Anal. Chem.* **2008**, *80*, 1883–1890.
[25] M. S. Wilson, *Anal. Chem.* **2005**, *77*, 1496–1502.
[26] S. Zhang, X. Li, F. Zhang, *Electrophoresis* **2007**, *28*, 4427–4434.
[27] Y. W. Cao, R. Jin, C. A. Mirkin, *Science* **2002**, *297*, 1536–1540.
[28] M. Han, X. Gao, J. Su, S. Nie, *Nat. Biotechnol.* **2001**, *19*, 631–635.
[29] B. Reiss, L. He, I. Walton, R. Cromer, C. Keating, M. Natan, *Science* **2001**, *294*, 137–141.
[30] J. A. Hansen, R. Mukhopadhyay, J. Hansen, K. V. Gothelf, *J. Am. Chem. Soc.* **2006**, *128*, 3860–3861.
[31] J. Miao, Z. Cao, Y. Zhou, C. Lau, J. Lu, *Anal. Chem.* **2008**, *80*, 1606–1613.
[32] J. A. Hansen, J. Wang, A. N. Kawde, Y. Xiang, K. V. Gothelf, G. Collins, *J. Am. Chem. Soc.* **2006**, *128*, 2228–2229.
[33] J. Elbaz, B. Shlyahovsky, R. Gill, D. Li, I. Willner, *ChemBioChem* **2008**, *9*, 232–239.
[34] Y. Du, B. Li, H. Wei, Y. Wang, E. Wang, *Anal. Chem.* **2008**, *80*, 5110–5117.
[35] K. Hu, D. Lan, X. Li, S. Zhang, *Anal. Chem.* **2008**, *80*, 9124–9130.
[36] S. Zhang, J. Xia, X. Li, *Anal. Chem.* **2008**, *80*, 8382–8388.
[37] M. Cho, S. Lee, S. Y. Han, J. Y. Park, M. A. Rahmen, Y. B. Shim, C. Ban, *Nucleic Acids Res.* **2006**, *34*, e75.
[38] J. Liu, J. H. Lee, Y. Lu, *Anal. Chem.* **2007**, *79*, 4120–4125.
[39] Z. Csoma, E. Huszar, E. Vizi, G. Vass, Z. Szabo, I. Herjavecz, M. Kollai, I. Horvath, *Eur. Respir. J.* **2005**, *25*, 873–878.
[40] P. Dolezalova, J. Krijt, J. Chladek, D. Nemcova, J. Hoza, *Rheumatology* **2005**, *44*, 74–79.
[41] R. C. Becker, F. A. Spencer, *J. Thromb. Thrombolysis* **1998**, *5*, 215–229.
[42] M. A. Shuman, P. W. Majerus, *J. Clin. Invest.* **1976**, *58*, 1249–1258.
[43] G. Jie, B. Liu, H. Pan, J. J. Zhu, H. Y. Chen, *Anal. Chem.* **2007**, *79*, 5574–5581.
[44] D. Zhu, Y. Tang, D. Xing, W. R. Chen, *Anal. Chem.* **2008**, *80*, 3566–3571.
[45] J. M. Nam, S. I. Stoeva, C. A. Mirkin, *J. Am. Chem. Soc.* **2004**, *126*, 5932–5933.
[46] S. Zhang, H. Zhong, C. Ding, *Anal. Chem.* **2008**, *80*, 7206–7212.
[47] A. Bini, M. Minunni, S. Tombelli, S. Centi, M. Mascini, *Anal. Chem.* **2007**, *79*, 3016–3019.
[48] S. Centi, S. Tombelli, M. Minunni, M. Mascini, *Anal. Chem.* **2007**, *79*, 1466–1473.

Received: June 23, 2009
Revised: July 31, 2009
Published online: December 10, 2009

